



Infrared microthermometry of fluid inclusions in transparent to opaque minerals: challenges and new insights

Hong-Wei Peng^{1,2} · Hong-Rui Fan^{1,2,3}  · M. Santosh^{4,5} · Fang-Fang Hu^{1,2,3} · Peng Jiang⁶

Received: 7 August 2018 / Accepted: 17 December 2019 / Published online: 8 January 2020
© Springer-Verlag GmbH Germany, part of Springer Nature 2020

Abstract

Infrared (IR) studies of fluid inclusions in opaque minerals provide direct insights into the ore-forming fluids. However, the challenge posed by the “warming effect” of IR light during microthermometry remains unresolved. Here we address this problem and show that the deviation in temperature of phase changes within fluid inclusions caused by IR light is more common than what was thought before. Our results reveal that transparent to translucent minerals (e.g., quartz, sphalerite) also absorb IR energy. Since IR absorption is influenced by the host mineral, the fluid inclusions hosted by different minerals exhibit different degrees of deviation in temperature during microthermometry. The Fourier transform infrared (FTIR) spectra do not display a consistent correlation between the band gap energy of a mineral and its absorption of IR energy. Minerals with low band gap energy, such as pyrite, absorb limited IR energy, resulting in small deviations of fluid inclusion data. In contrast, this deviation could be significant for fluid inclusions hosted in minerals with a relatively high band gap energy, such as iron-rich sphalerite and wolframite. Substitution of iron increases the absorption of IR energy in these minerals. The substitution of trace elements may also play a role. Our quantitative analyses confirm that using the lowest possible IR light intensity with the smallest diaphragm minimizes the “warming effect” of IR light. We also propose an improved cycling method as a better option where high IR light intensity is required.

Keywords Infrared microscope · Deviation of IR microthermometry · Absorption of IR light energy · FTIR · Major and trace element substitution · Improved cycling method

Editorial handling: R. Moritz

Electronic supplementary material The online version of this article (<https://doi.org/10.1007/s00126-019-00950-z>) contains supplementary material, which is available to authorized users.

✉ Hong-Rui Fan
fanhr@mail.iggcas.ac.cn

¹ Key Laboratory of Mineral Resources, Institute of Geology and Geophysics, Chinese Academy of Sciences, Beijing 100029, China

² College of Earth and Planetary Sciences, University of Chinese Academy of Sciences, Beijing 100049, China

³ Institutions of Earth Science, Chinese Academy of Sciences, Beijing 100029, China

⁴ School of Earth Sciences and Resources, China University of Geosciences Beijing, 29 Xueyuan Road, Beijing 100083, China

⁵ Department of Earth Science, University of Adelaide, Adelaide, SA 5005, Australia

⁶ Department of Geological Sciences, University of Florida, Gainesville, FL 32611, USA

Introduction

Fluid inclusions trapped in minerals provide direct insights into the physicochemical conditions of hydrothermal fluids (e.g., Roedder 1984; Goldstein and Reynolds 1994). Fluid inclusions in transparent gangue minerals, such as quartz, calcite, and fluorite, are commonly studied under visible light. The analytical procedures of fluid inclusions in transparent minerals are well established, and the reliability of microthermometric data is commonly accepted. However, fluid inclusions hosted by visible light opaque minerals are better choices to investigate the conditions of metal precipitation, because of the direct record of ore-forming fluids, and avoiding co-genetic assumption with mineralization for transparent gangue minerals in fluid inclusion studies (Campbell and Robinson-Cook 1987; Campbell and Panter 1990; Wilkinson 2001; Lüders 2017). Recently, infrared (IR) studies on fluid inclusions were carried out on wolframite, stibnite, enargite, hematite, dark sphalerite, and pyrite (e.g., Kouzmanov et al. 2010; Shimizu and Morishita 2012; Wei

et al. 2012; Zhu et al. 2013; Ni et al. 2015; Takács et al. 2017; Korges et al. 2018; Casanova et al. 2018; Ortelli et al. 2018). However, the accuracy of IR microthermometry is still questioned, since the IR light may cause variations of microthermometric data (e.g., Moritz 2006).

Possible discrepancies in microthermometric results between IR and visible light were considered since the first IR research on fluid inclusions in wolframite (Campbell and Robinson-Cook 1987; Campbell and Panter 1990). Fluid inclusions in several minerals (i.e., sphalerite, quartz, huebnerite, and fluorite), which are semi-transparent to transparent under both IR and visible light, were measured for the temperature of ice melting (T_m) and the temperature of homogenization (T_h) under IR and visible light. Good correlations of the results of T_m and T_h under both light settings were obtained (Campbell and Robinson-Cook 1987; Campbell and Panter 1990; Bailly et al. 2000, 2002; Shimizu et al. 2003; Shimizu and Morishita 2012). Rosière and Rios (2004) reported that no temperature variation was observed in hematite during IR analysis, even under IR light longer than 1 h during measurements. Lindaas et al. (2002) tested one fluid inclusion in fluorite five times, and found a standard deviation of T_m was ± 0.4 °C using the USGS gas-flow heating/freezing stage. When using Linkam heating/freezing stage, the standard deviation was only ± 0.1 °C. The aforementioned examples were thought to be evidence confirming the accuracy of the IR analytical results, and demonstrating that IR light had no influence on the microthermometric data.

However, during IR microthermometric studies of fluid inclusions in enargite, Moritz (2006) found that the measured T_m and T_h decreased dramatically as the IR light intensity increased, which resulted in underestimating T_h and overestimating salinities of fluid inclusions. It was concluded that IR light energy was likely absorbed by the host mineral. A similar result was also reported for stibnite by Ge et al. (2011), and Casanova et al. (2018) observed similar phenomena for fluid inclusions hosted by different opaque minerals.

If one accepts that visible light opaque minerals can absorb more IR energy than semi-transparent to transparent minerals, it would be reasonable to infer that IR light can cause greater deviations in pyrite microthermometric data, as pyrite has a smaller band gap energy and a higher wavelength of absorption edge than enargite and stibnite (Campbell 1991; Lüders 2017). Thus, fluid inclusions in pyrite were not measured in the study of Kouzmanov et al. (2010). However, Zhu et al. (2013) measured T_m and T_h of several fluid inclusions hosted by pyrite and the deviations were 0.3 °C for T_m and 0.3 to 1.3 °C for T_h . The small variations were thought to prove the limited influence of IR light during microthermometry of fluid inclusions in pyrite, and to support the accuracy of the microthermometric data.

Thus, previous studies provide contradictory conclusions on accuracy of IR microthermometry. Even though Moritz

(2006) recommended using the lowest possible IR light intensity with all diaphragms nearly closed, the possible heating influence from IR light and the deviation of microthermometric data cannot be excluded. Furthermore, high IR light intensity is usually necessary for studies of minerals with low IR transparency. Laser ablation-inductively coupled plasma-mass spectrometry (LA-ICP-MS) combined with IR microscopy has been employed to study the composition of hydrothermal fluids, where salinities of fluid inclusions hosted by opaque minerals were used as an internal standard (Kouzmanov et al. 2010; Korges et al. 2018). In this case, accurate IR microthermometric measurements of fluid inclusion is a prerequisite for the accuracy of the LA-ICP-MS results.

The causes for the variations in the temperature of phase change under IR illumination have not been sufficiently explored in previous studies. Some researchers suggested absorbance of IR light by the host mineral (e.g., Moritz 2006; Casanova et al. 2018). However, water (H_2O) and carbon dioxide (CO_2) in fluid inclusions have a strong absorption band in the IR range (Campbell and Robinson-Cook 1987), which suggests that fluid inclusion themselves may play a role in absorbing the IR energy. Besides, the silver lid in the Linkam freezing/heating stage was thought to cause warming (Lüders 2017), and the illumination time of IR light during measurements of fluid inclusions in hematite was used to prove the lack of influence of IR light on microthermometric results (Rosière and Rios 2004). However, the possible roles of these factors in absorbing IR energy are still not well confirmed.

In this study, we attempt to quantitatively evaluate the deviation of phase change temperatures of fluid inclusions caused by IR light. For this purpose, different types of fluid inclusions hosted by visible light transparent to opaque minerals are examined. We also design experiments to evaluate the role of possible factors in absorbing the IR energy (e.g., host minerals, fluid inclusion chemistry, silver lid, and illumination time). The deviation of microthermometric data of fluid inclusion, using the lowest possible IR light intensity, with the smallest field iris diaphragm, is also investigated.

Analytical method and sample preparation

Equipment

Optical observations were conducted using an Olympus BX53 IR microscope equipped with a Qimaging Retiga-2000R digital CCD camera and a Dage-MTI LSC-70 tube camera for fluid inclusions in visible light transparent to opaque minerals. The brightness adjustment and the brightness marks, which divides the voltage of the bulb of the microscope, were utilized to set the IR light intensities (ESM Fig.

S1). The field iris diaphragm was used to control the diaphragm size (ESM Fig. **S1**). Microthermometries of fluid inclusions were conducted using a Linkam THMSG 600 heating/freezing stage. The near-infrared absorption spectra of the mineral sections were obtained using a Bruker Vertex 70-V FTIR spectrometer, which is connected with a Bruker Hyperion 2000 microscope for in situ analysis. The major, minor, and trace element contents of sphalerite, stibnite, and pyrite were determined by a JEOL JXA-8100 electron probe microanalyzer (EPMA). The trace element analyses of quartz by LA-ICP-MS were performed, using an Agilent 7900 ICP-MS equipped with a GeoLasPro 193 nm ArF excimer laser. More detailed information of the equipment and the calibration of the microthermometric stage are given in the ESM-1.

Sample selection and preparation

Quartz samples used in this study were collected from the Majiayao (MJY) gold deposit in the Jiaodong gold province in eastern China, and the Yaogangxian (YGX) and Jiagangxueshan (JGXS) tungsten deposits in south China. The fluorite samples were collected from the Penglai fluorite deposit, Jiaodong. Dark and light brown sphalerites (DBS and LBS) were chosen from the Boltsburn Mine in UK and Shuikoushan lead-zinc deposit in south China, respectively. The stibnite samples are from the Xikuangshan (XKS) and Qinglong (QL) antimony deposits in southwest China, and the wolframite samples were selected from the Yaogangxian and Jiagangxueshan tungsten deposits. The pyrite samples come from the Linglong (LL) gold deposits in Jiaodong, and the Yinjiagou (YJG) deposit in central China, which were also described by Zhu et al. (2013).

Samples with euhedral-subhedral crystals were selected to prepare 74 doubly polished sections. The thickness of quartz, fluorite, and sphalerite sections are approximately 300 μm , whereas the stibnite and wolframite sections are thinner, ranging from 100 to 200 μm . The pyrite sections range in thickness from ca. 80 to 150 μm . Both sides of all sections were polished well to optimize the transparency, which is particularly important for opaque mineral microthermometry.

Analytical procedures

The basic experimental method was similar to that of Moritz (2006) who used only enargite for his fluid inclusion investigation. In the present study, however, we chose minerals with different visible and IR light transparencies to investigate the role of mineral type in absorbing the IR light energy. Temperatures of phase change of fluid inclusions in transparent to translucent minerals were measured using different IR light intensities (intensities of 5 and 10 for fluid inclusions in quartz and fluorite, and 2, 4, 6, 8, and 10 for fluid inclusions in sphalerite) and under visible light. Microthermometry was

conducted for fluid inclusions in opaque minerals (stibnite, wolframite, and pyrite) under relative IR light intensities of 2, 4, 6, 8, and 10, and at 3, 5, and 10 intensity with the smallest diaphragm opening.

The standard synthetic two-phase liquid-rich pure H_2O and three-phase CO_2 -rich fluid inclusions, two-phase liquid-rich fluid inclusions with different salinities and compositions, and three-phase CO_2 -rich fluid inclusions in quartz and sphalerite were chosen to constrain the possible effects of fluid inclusion components in absorbing the IR energy. Temperatures of ice melting and of homogenization of two-phase liquid-rich fluid inclusions, and phase changes of CO_2 in three-phase CO_2 -rich fluid inclusions, were measured under 5 and 10 IR relative light intensities and under visible light.

Some fluid inclusions in sphalerite, stibnite, and wolframite were measured twice under the same IR light intensities. The only difference between the two analyses was the illumination time under IR light during the heating to T_m . Microthermometric data of fluid inclusions in wolframite were obtained twice, with and without a silver lid covered on, to check whether warming by IR light is associated with the silver lid.

In order to quantitatively evaluate the deviation of fluid inclusion microthermometry in opaque minerals, it is necessary to obtain the accurate values of T_m and T_h without the influence of IR radiation. Thus, we improved the cycling method after Goldstein and Reynolds (1994) to obtain a result unaffected by IR heating. Figure 1 shows an example of the improved cycling method where the T_m of the fluid inclusion is between -3.5 and -3.0 $^\circ\text{C}$. During each round of heating, the IR light was turned off, and after heating to the target temperature, the IR light was turned on to observe the volume changes of bubble and ice in the fluid inclusion during the subsequent rapid cooling. Compared with previous studies which applied the cycling method to IR microthermometry (Lüders and Ziemann 1999; Lindaas et al. 2002), the values of T_m and T_h obtained applying this improved cycling method are considered to be true values without the influence of IR radiation, because IR light was turned off during each round of heating. The heating interval of each round was maintained at 0.1 $^\circ\text{C}$.

Following the microthermometry, FTIR and EPMA, as well as LA-ICP-MS analyses, were performed on the same areas of the mineral sections, where fluid inclusions were measured.

Results

Fluid inclusion petrography

In the present study, we selected the largest and flattest fluid inclusions so that the phase changes could be easily observed. The measured two-phase liquid-rich, and three-phase CO_2 -

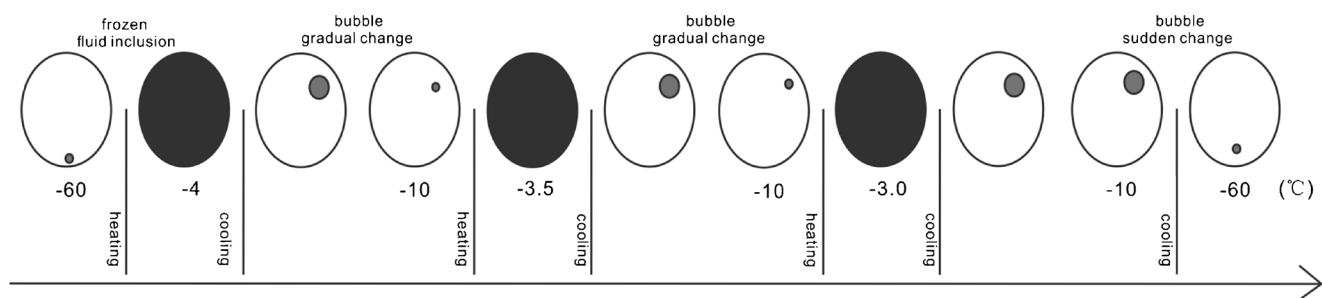


Fig. 1 Improved cycling technique of IR microthermometry used for determining the phase change temperatures of fluid inclusions without the influence of IR light (modified after Goldstein and Reynolds 1994). The sketch shows an example of temperature of ice melting between -3.5

and -3.0 °C. The arrow shows the evolution of time. The black fluid inclusions represent conditions with the IR light turned off during heating, and after reaching the target temperature, the IR light is turned on during subsequent rapid cooling (white fluid inclusion)

rich, fluid inclusions in quartz form negative crystals with rounded and irregular shape, and mostly range in size from 8 to 30 μm (Fig. 2a, b). In fluorite, only two-phase liquid-rich inclusions were found, with a negative crystal to rounded shape and showing a size range of 10 to 40 μm (Fig. 2c). The two-phase liquid-rich fluid inclusions in sphalerite are

relatively irregular in shape, suggesting significant post-trapping modification (Fig. 2d). The analyzed fluid inclusions in sphalerite were generally 20 to 100 μm in size (Fig. 2d–f).

In stibnite, wolframite and pyrite, only two-phase liquid-rich fluid inclusions were found. The measured fluid inclusions in stibnite and wolframite were tubular or flat and ranged

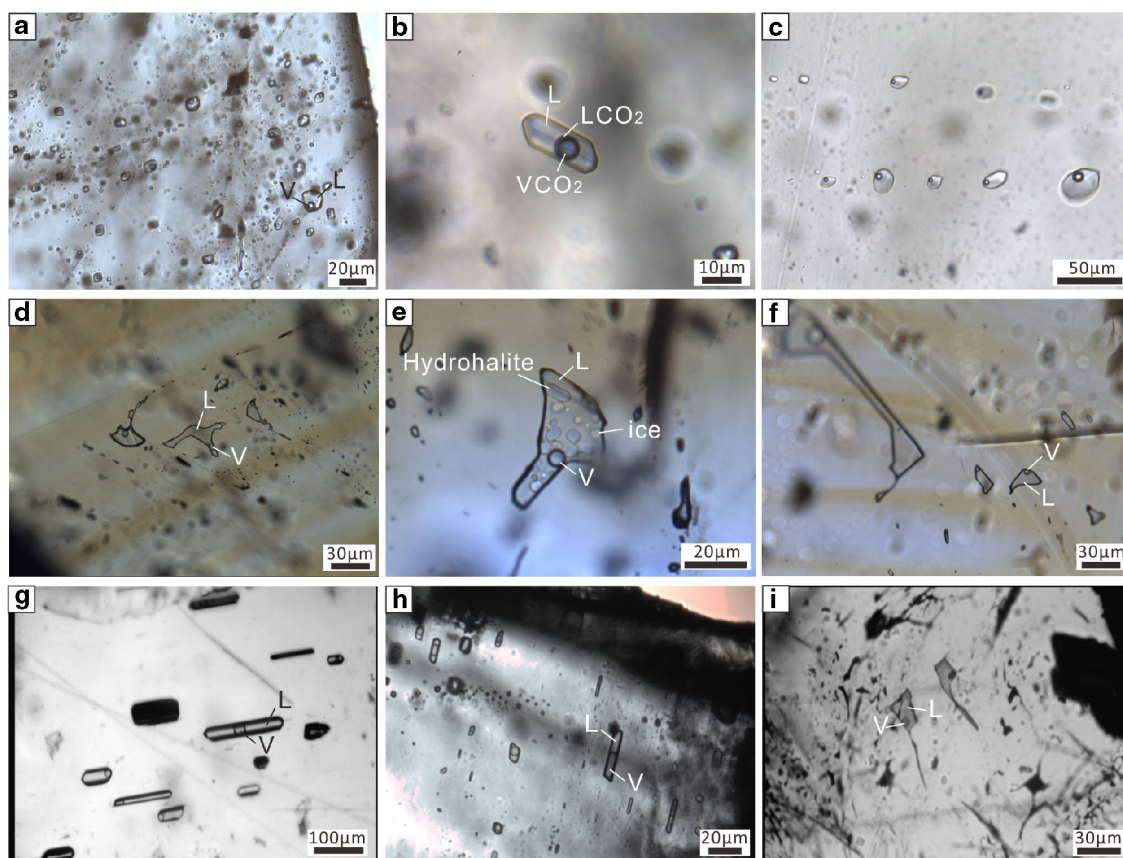


Fig. 2 Photomicrographs of measured fluid inclusions in transparent to opaque minerals. **a** Two-phase liquid-rich fluid inclusions in Yaogangxian quartz. **b** Three-phase CO_2 -rich fluid inclusion in quartz from the Majiayao deposit. **c** Measured fluorite fluid inclusions from the Penglai deposit. **d** Two-phase liquid-rich fluid inclusions in sphalerite with dark brown color from the Boltsburn Mine. **e** Fluid inclusion with a composition belonging to $\text{H}_2\text{O}-\text{NaCl}-\text{CaCl}_2$ system in dark brown

sphalerite from the Boltsburn Mine. Crystals of hydrohalite and ice were observed during heating to T_m . **f** Two-phase liquid-rich fluid inclusions in light brown color sphalerite from the Shuikoushan deposit. **g** Two-phase liquid-rich fluid inclusions with a negative crystal shape in Qinglong stibnite. **h** Two-phase liquid-rich fluid inclusions in Jiagangxueshan wolframite. **i** Two-phase liquid-rich fluid inclusions in Linglong pyrite

in size from 25 to 120 μm , and 5 to 40 μm , respectively (Fig. 2g, h). The fluid inclusions in pyrite were flat and irregular, ranging in length from 40 to 60 μm (Fig. 2i).

Transparency of stibnite, wolframite, and pyrite under IR light

Samples of stibnite and wolframite exhibit good transparency, although a few samples from the same deposit have poor transparency. Within the same mineral section with good transparency, some domains show patchy or zoned transparency. Pyrite generally has variable IR transparency in different regions of one section, and even within one grain of pyrite, with the band patterns showing different transparency corresponding to heterogeneous distribution of trace elements (Richards and Kerrich 1993; Kouzmanov et al. 2002; Orтели et al. 2018). However, most fluid inclusions were located in domains with good IR transparency. The grain boundaries and fractures can cause opaque areas, and thus, euhedral and large mineral grains have better IR transparency than the fine-grained aggregates. The transparency of pyrite and wolframite gradually decreased during heating, which is attributed to the shift of the main absorption edge toward longer wavelengths (Lüders and Ziemann 1999; Lindaas et al. 2002; Lüders 2017).

Deviation of microthermometric results caused by IR light

The term deviation in this study refers to difference between microthermometric results of fluid inclusions under IR and visible light. The deviation thus equals $\text{value}_{\text{visible light}} - \text{value}_{\text{IR10}}$ or $\text{value}_{\text{cycling}} - \text{value}_{\text{IR10}}$, and is expressed as the mean value of deviation of a group of fluid inclusions which are spatially associated and measured.

The IR microthermometric results show that the temperatures of phase changes decrease as the IR light intensity increases (Fig. 3a–c). Notably, the rate of the deviation change increases as the light intensity increases. The co-variation of the fluid inclusion microthermometric data and light intensity defines a curve (e.g., Fig. 3b), which is different from previous studies which reported a nearly linear relation (Moritz 2006; Ge et al. 2011). When using the smallest diaphragm, the degree of variations and the change in the fluid inclusion data are much smaller (Fig. 3a–c).

The IR microthermometric data of fluid inclusions in different minerals at high and low temperatures show almost identical deviations, even though some fluid inclusions display smaller deviations of Th compared with the deviations of Tm (ESM Tables S2-4 to S2-11). Considering the lower accuracy of the heating/freezing stage at high temperature, and that fluid inclusions were cooled first and then heated, the results of phase changes at low temperatures are thought to

be more reliable. In addition, when studying fluid inclusions in opaque minerals, the bubble sometimes did not reappear following rapid cooling after the first homogenization. Thus, in the following sections, we mainly use the results of phase changes at low temperatures.

In this study, when a group of spatially associated fluid inclusions were analyzed together, they yielded the same degree of deviation of phase change temperatures caused by IR radiation, which are shown by parallel curves in Fig. 3 a–c, Fig. 4 a and c, and Fig. 6 a. Fluid inclusions hosted by the same mineral but in different samples (e.g., fluid inclusions in Yaogangxian and Jiagangxueshan wolframite) and fluid inclusions within different areas of the same mineral section (e.g., fluid inclusions in sphalerite samples) show different degrees of deviation (Figs. 3b; 4a, c; 5a; 6a).

Synthetic fluid inclusion standard

Eight two-phase liquid-rich pure H_2O , and four three-phase CO_2 -rich synthetic fluid inclusions, were measured under visible and IR light intensities of 5 and 10. The phase changes of Tm_{CO_2} , Tm_{CLA} , and Th_{CO_2} of three-phase CO_2 -rich inclusions, and Tm of two-phase liquid-rich pure H_2O inclusions, show variations within 0.1 $^\circ\text{C}$. The largest deviation of Th of two-phase liquid-rich pure H_2O inclusions is 0.2 $^\circ\text{C}$, which is smaller than the systematic analytical error of ± 0.5 $^\circ\text{C}$ for five successive analyses.

Quartz

Our study shows that fluid inclusion data in quartz can be influenced by IR light, which has not been reported before. The deviations of fluid inclusion microthermometric data caused by IR radiation are 1.0–1.4 $^\circ\text{C}$ (fluid inclusions in Majiayao quartz; ESM Table S2-6), 0.4–0.6 $^\circ\text{C}$ (fluid inclusions in Jiagangxueshan quartz; ESM Table S2-7), and 0.1–0.2 $^\circ\text{C}$ (fluid inclusions in Yaogangxian quartz; ESM Table S2-8). In addition, the Majiayao and Jiagangxueshan three-phase CO_2 -rich fluid inclusions show almost the same deviations of IR microthermometric data as the two-phase, liquid-rich, fluid inclusions (ESM Tables S2-6 and S2-7).

Fluorite

Thirteen fluid inclusions were studied in fluorite. The only discernible difference of phase change temperatures caused by IR radiation is 0.1–0.2 $^\circ\text{C}$ (ESM Table S2-9). Considering instrumental error, this deviation is thought to be negligible.

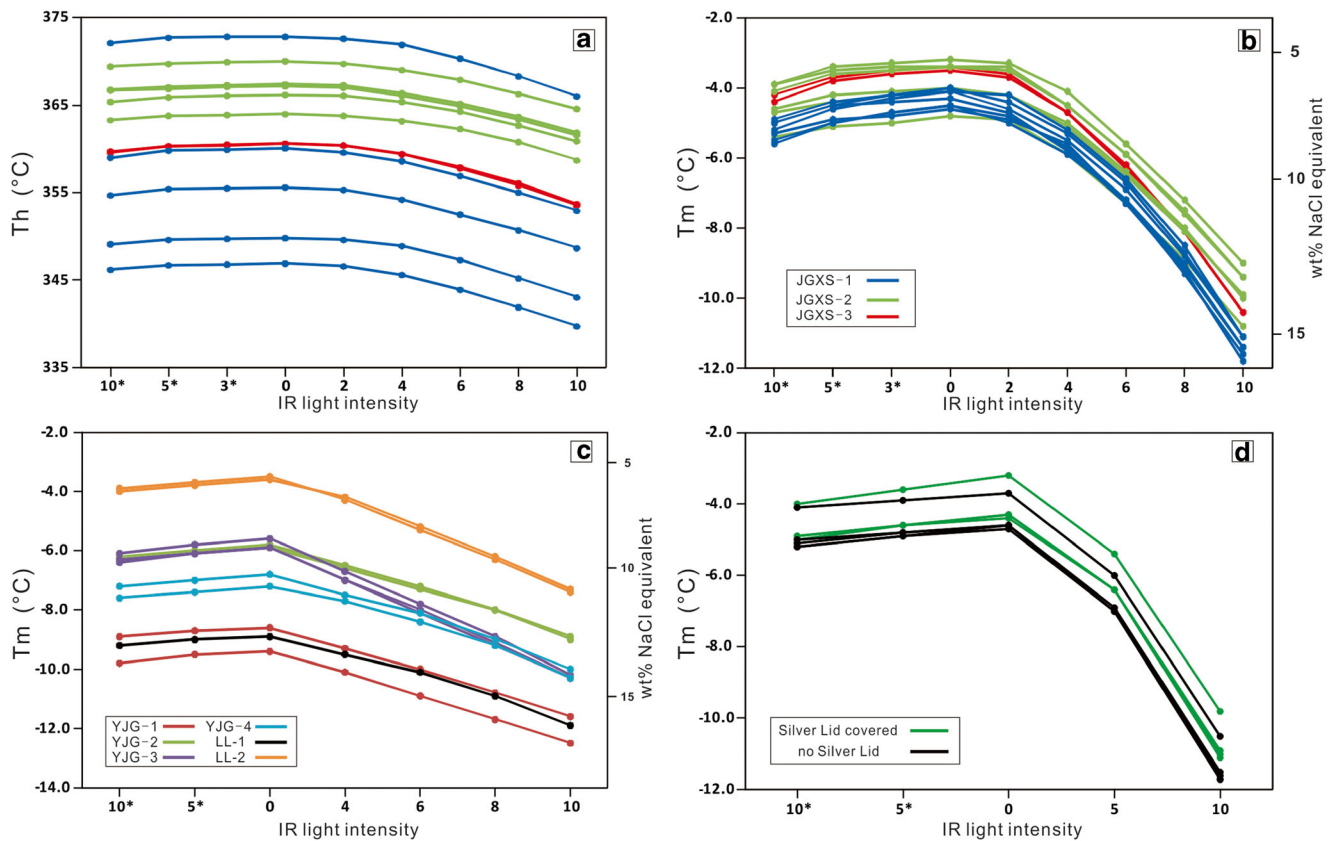


Fig. 3 **a** Th and **b** Tm IR microthermometric data of three groups of wolframite fluid inclusions from the Jiagangxueshan deposit. **c** Tm IR measurement results of Yinjiagou and Linglong fluid inclusions hosted by pyrite. **d** Infrared analyses results of Jiagangxueshan wolframite fluid inclusions using a silver lid covered in the Linkam freezing/heating stage and without silver lid, respectively. The symbol “*” represents

measurement using the smallest possible diaphragm opening. The results of IR light intensity of “0” were obtained using the improved cycling method. Curves with the same color represent a group of adjacent fluid inclusions measured simultaneously, and curves with different colors mean different groups of fluid inclusions

Sphalerite

Three groups of fluid inclusions from different areas in one dark brown sphalerite (DBS) section and in one light brown sphalerite (LBS) section were measured. In the DBS section, three groups of fluid inclusions (DBS-1, DBS-2, and DBS-3) display deviations of Tm of 2.7 °C, 4.3 °C, and 1.5 °C, respectively (Fig. 4a; ESM Table S2-10). The three fluid inclusion groups (LBS-1, LBS-2, and LBS-3) display Tm deviations of 0.3 °C, 0.4 °C, and 1.1 °C, respectively (Fig. 4c; ESM Table S2-11). During heating, some fluid inclusions in DBS showed phase changes corresponding to the H₂O–NaCl–CaCl₂ system, with a eutectic temperature lower than –50 °C, and melting of hydrohalite at a temperature lower than –21.2 °C, followed by the melting of ice (Fig. 2e; ESM Table S2-10). One H₂O–NaCl fluid inclusion and one H₂O–NaCl–CaCl₂ fluid inclusion were analyzed together and yielded the same deviations (Fig. 4a).

Wolframite

Three groups of fluid inclusions in wolframite from the Jiagangxueshan and Yaogangxian deposits were studied.

The fluid inclusions of the Yaogangxian wolframite (YGX-1, YGX-2, and YGX-3) yielded Tm deviations of 10.0 °C, 9.2 °C, and 10.6 °C (Fig. 5a; ESM Table S2-5), which are greater than those in samples from the Jiagangxueshan deposit (JGXS-1, JGXS-2, and JGXS-3) with deviations of 7.1 °C, 5.9 °C, and 7.0 °C (Fig. 5a; ESM Table S2-4). One group of fluid inclusions in the Jiagangxueshan wolframite was measured twice with, and without, the silver lid yielding deviations of 6.7 °C and 7.0 °C, respectively (Fig. 3d; ESM Table S2-14).

Stibnite

Three groups of fluid inclusions in stibnite from the Xikuangshan deposit and one group of fluid inclusions in stibnite from the Qinglong deposit were studied. The Tm deviations of the three groups of measurements of the Xikuangshan stibnite (XKS-1, XKS-2, and XKS-3) are 4.6 °C, 3.2 °C, and 4.1 °C, whereas the stibnite fluid inclusions from Qinglong display deviations of 2.3 °C (Fig. 6a; ESM Table S2-12).

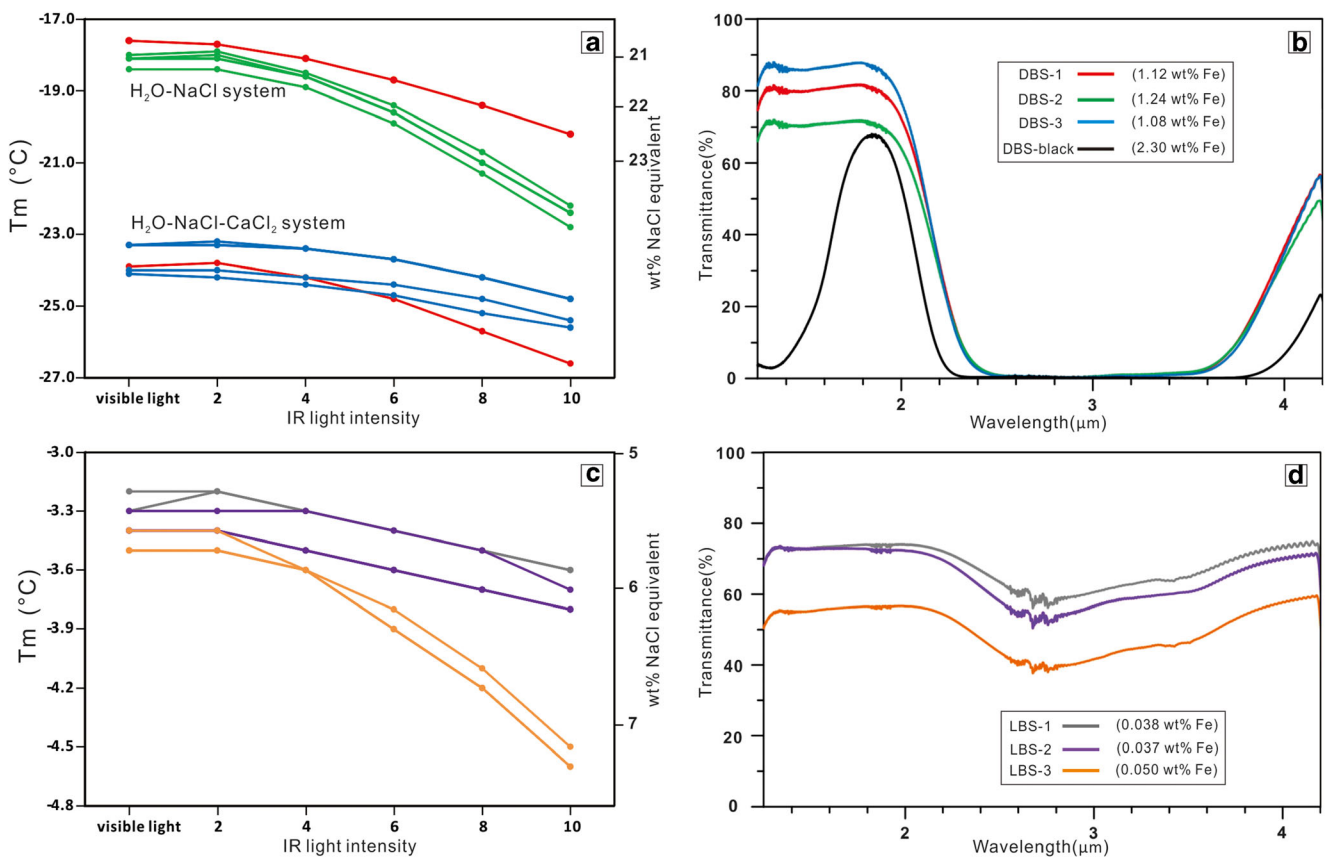


Fig. 4 **a** Infrared Tm data of three groups of fluid inclusion from different areas in one DBS section from the Boltshurn mine. **b** FITR spectra of the three DBS samples in Fig. 4a. **c** Infrared Tm measurement data of three

groups of fluid inclusions from different areas in one LBS section from the Shuikoushan deposit. **d** FITR spectra of the three LBS samples in Fig. 4c

Pyrite

Microthermometric studies of fluid inclusions in pyrite from the Yinjiagou and Linglong deposits (Fig. 3c) show relatively small deviations compared to the wolframite

fluid inclusions (Fig. 3b). Four groups of fluid inclusions in Yinjiagou pyrite (YJG-1, YJG-2, YJG-3, and YJG-4) yielded Tm deviations of 3.0 °C, 3.1 °C, 4.5 °C, and 3.1 °C, respectively, and two groups of fluid inclusions in pyrite from the Linglong deposit (LL-1 and LL-2) display

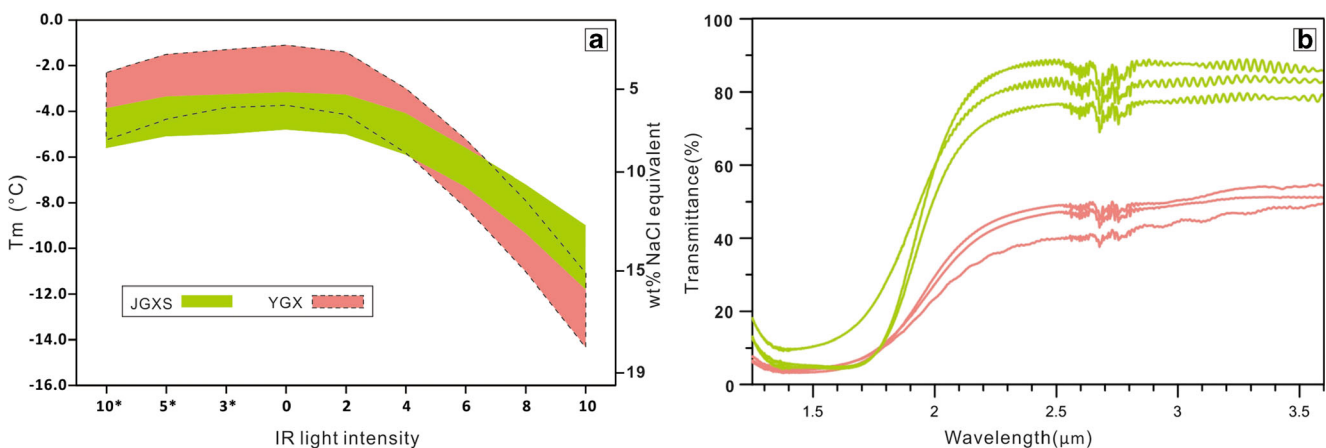


Fig. 5 **a** Infrared Tm microthermometric data of fluid inclusions in wolframite from the Jiagangxueshan and Yaogangxian deposits. Three groups of fluid inclusions from Jiagangxueshan and Yaogangxian samples were measured. The symbol “*” represents measurements

using the smallest possible diaphragm opening. The results of IR light intensity of “0” were measured by the improved cycling method. **b** FITR spectra of wolframite

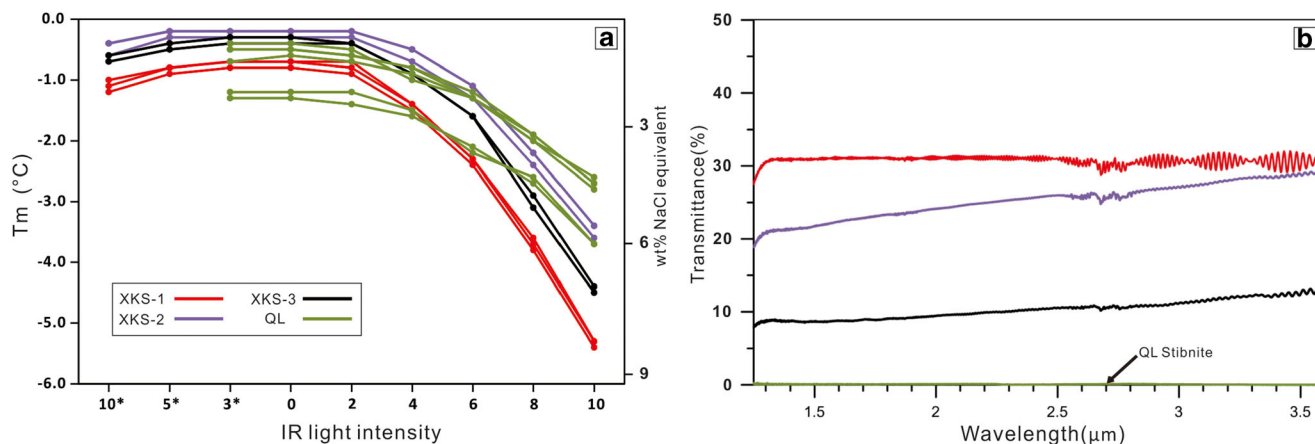


Fig. 6 **a** Infrared T_m microthermometric data of fluid inclusions in stibnite from Xikuangshan and Qinglong deposits. The symbol “*” represents measurements using the smallest possible diaphragm

opening. The results of IR light intensity of “0” were measured by the improved cycling method. **b** FTIR spectra of the stibnite

T_m deviations of 3.8 °C and 3.0 °C, respectively (Fig. 3c; ESM Table S2-13).

Infrared spectra of sphalerite, wolframite, and stibnite

The infrared spectra were analyzed in situ using FTIR in sphalerite, stibnite, and wolframite, which were studied by IR microthermometry. The results show a clear difference with deviations.

In sphalerite, there are notable distinctions in the FTIR spectra between the DBS and the LBS (Fig. 4b, d). The IR transmittance of DBS decreases sharply and becomes opaque between wavelength (λ) of 2.4 and 3.6 μm , whereas the spectra of the LBS shows only a slight decrease in this wavelength range, still with good transmittance. They both present constant and relatively high IR transmittance in the wavelength range between 1.3 and 2 μm . In one section, the group of fluid inclusions with the highest deviation of IR fluid inclusion data has the lowest IR transmittance, and the group with the lowest deviation shows the highest IR transmittance (Fig. 4). This relationship can be noticed in both types of sphalerite. Furthermore, a black area in the DBS section has a much lower IR transmittance in the λ range of 1.3 and 2 μm , compared with the DBS-1, DBS-2, and DBS-3.

The FTIR spectra of wolframite shows an increase of IR transmittance at $\lambda=1.7$ μm and an increase of IR transmittance toward shorter wavelength at $\lambda=1.3$ μm (Fig. 5b), which is consistent with the reported two maxima of IR transmittance of wolframite samples

(Lüders 2017). The wolframite samples from the Yaogangxian deposit, with larger deviations of IR microthermometric results, show lower IR transmittance and longer absorption edges than Jiagangxueshan wolframite, which have smaller deviations (Fig. 5a, b).

The FTIR spectra of stibnite exhibit smoother patterns, similar to the results of previous studies (Fig. 6b; Lüders 2017). The Qinglong stibnite shows lower IR transmittance in the FTIR spectrum compared with Xikuangshan stibnite (Fig. 6b), although both of them are transparent under IR light (Figs. 2g and 7e). The Qinglong stibnite section (ca. 200 μm) in thickness is much thicker than the Xikuangshan stibnite (ca. 100 μm). The significant difference in thickness likely results in their different IR transmittance in FTIR spectra.

Major, minor, and trace element contents of host minerals

Quartz

Quartz studied by microthermometry was analyzed by LA-ICP-MS for trace element contents and the results are listed in the ESM Table S2-1. A total of 30 spots were analyzed, among which 26 spots yielded good signals enabling the calculation of average trace element contents of quartz in samples from the Majiayao, Jiagangxueshan, and Yaogangxian deposits. The quartz samples from these three deposits do not show any significant differences in trace element contents. The main

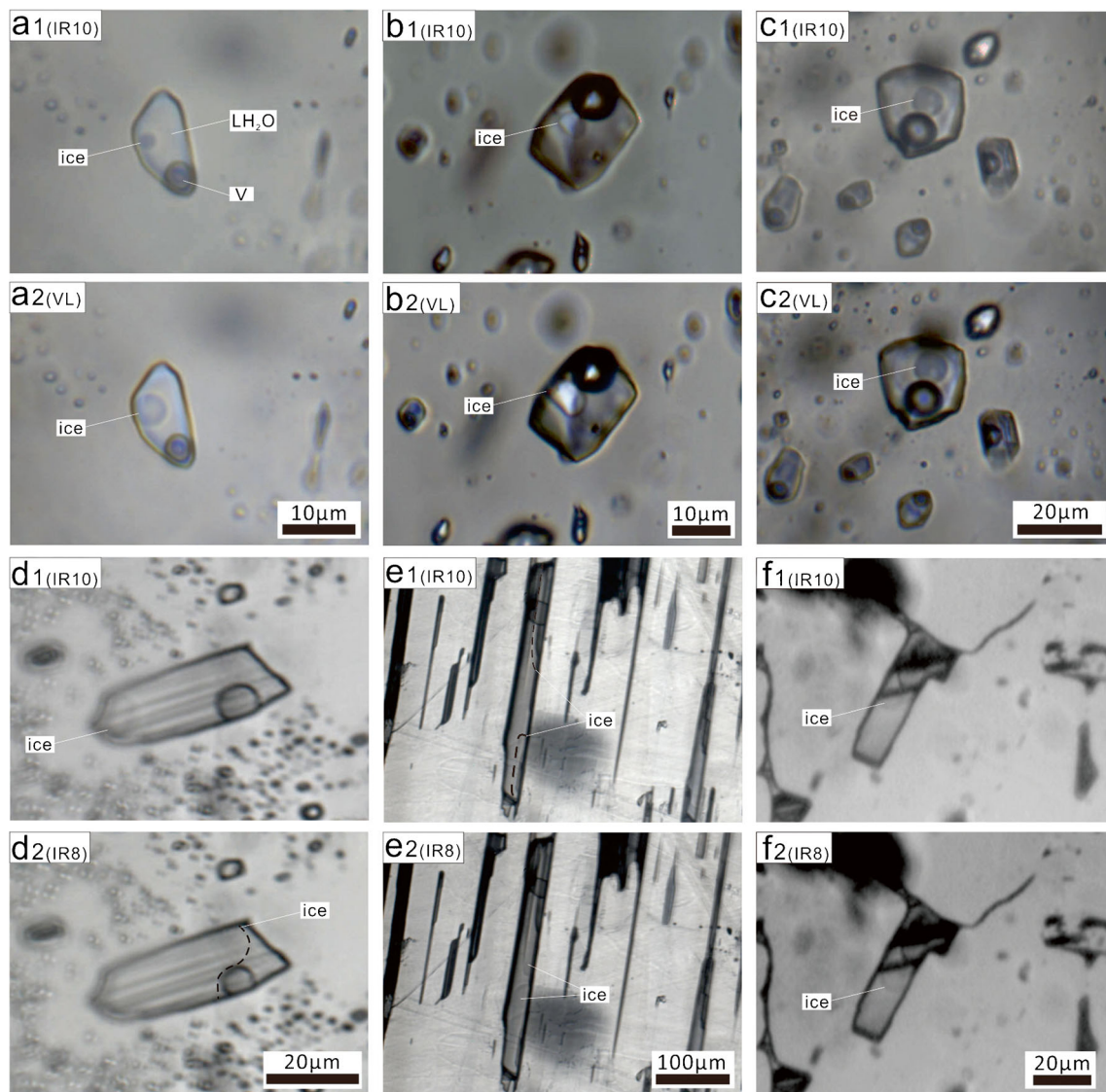


Fig. 7 The size of remnant ice in fluid inclusion is sensitive to the change of light conditions at constant temperature. **a–c** Quartz fluid inclusions from Majiayao, Jiagangxueshan, and Yaogangxian, respectively. a1, b1, and c1 were taken with an IR light intensity of 10 (IR10), whereas a2, b2,

and c2 were taken under visible light (VL). **d–f** fluid inclusions trapped in wolframite, stibnite, and pyrite, respectively. d1, e1, and f1 were taken with an IR light intensity of 10, whereas d2, e2, and f2 were taken under light intensity of 8 (IR8)

trace element variations are detected for Li, Al, P, Ca, and Ti (ESM Table S2-1).

Although some elements (e.g., Na and K) display large difference in concentration, the contents of Na and K are scattered. The spots having high Na and K contents are contributed to fluid inclusion in quartz. Some other elements (e.g., As, Se, and Ag) also exhibit variable concentrations. Most of the analyzed spots have very low concentrations and the spots with high concentration likely represent signals from mineral or fluid inclusions not

deleted before analysis, and are therefore not considered in this study.

Sphalerite

The major, minor, and trace element contents of the three plates (DBS-1, DBS-2, DBS-3) separated from a DBS section and the three plates (LBS-1, LBS-2, LBS-3) separated from a LBS section were analyzed by EPMA at the same locations where fluid inclusions were measured. The results are listed in Table 1

Table 1 Average contents of major, minor, and trace elements of sphalerite, stibnite, and pyrite (wt%), measured by EPMA

Mineral	Sample No.	Spot	Fe	Zn	Sb	S	As	Pb	Au	Cu	Bi	Co	Ni	Ag	Se	Te	Total
Sphalerite	DBS-1	16	1.12	64.33	bdl	33.37	bdl	0.19	bdl	bdl	0.15	bdl	bdl	bdl	bdl	bdl	99.16
	DBS-2	15	1.24	64.28	bdl	33.26	bdl	0.25	bdl	bdl	0.11	bdl	bdl	bdl	bdl	bdl	99.14
	DBS-3	16	1.08	64.64	bdl	33.40	bdl	0.27	bdl	bdl	0.12	bdl	bdl	bdl	bdl	bdl	99.51
	DBS-black	3	2.30	63.31	bdl	33.16	bdl	0.21	bdl	0.03	0.07	bdl	bdl	bdl	bdl	bdl	99.08
	LBS-1	10	0.038	65.87	bdl	33.36	bdl	0.18	bdl	bdl	0.11	bdl	bdl	bdl	bdl	bdl	99.56
	LBS-2	16	0.037	66.04	bdl	33.23	bdl	0.25	bdl	bdl	0.13	bdl	bdl	bdl	bdl	bdl	99.69
	LBS-3	15	0.050	65.38	bdl	33.11	bdl	0.25	bdl	bdl	0.13	bdl	bdl	bdl	bdl	bdl	98.92
Stibnite	XKS-1	13	bdl	bdl	70.59	28.52	0.20	0.22	0.21	bdl	0.09	bdl	bdl	bdl	0.04	bdl	99.87
	XKS-2	10	bdl	bdl	70.45	28.48	0.18	0.18	0.15	bdl	0.10	bdl	bdl	0.02	bdl	bdl	99.56
	XKS-3	13	bdl	bdl	70.63	28.62	0.17	0.19	0.17	bdl	0.07	bdl	bdl	bdl	bdl	bdl	99.85
	QL	13	bdl	bdl	70.33	28.41	0.17	0.27	0.13	bdl	0.10	bdl	bdl	bdl	bdl	bdl	99.41
Pyrite	YJG-1	11	46.54	bdl	bdl	53.30	bdl	0.31	bdl	bdl	0.21	bdl	bdl	bdl	bdl	bdl	100.36
	YJG-2	12	46.53	bdl	bdl	53.66	bdl	0.43	bdl	bdl	0.18	bdl	bdl	bdl	bdl	bdl	100.80
	YJG-3	12	46.43	bdl	bdl	53.14	bdl	0.38	bdl	bdl	0.22	bdl	bdl	bdl	bdl	bdl	100.17
	YJG-4	12	46.49	bdl	bdl	53.15	bdl	0.36	bdl	bdl	0.21	bdl	bdl	bdl	bdl	bdl	100.21
	LL-1	12	46.24	bdl	bdl	52.98	bdl	0.32	bdl	bdl	0.20	bdl	bdl	bdl	bdl	bdl	99.74
	LL-2	12	46.50	bdl	bdl	53.23	bdl	0.34	bdl	bdl	0.18	bdl	bdl	bdl	0.04	bdl	100.29

bdl below the detection limit

DBS and LBS are dark brown sphalerite and light brown sphalerite, from Boltsburn Mine and Shuikoushan deposit respectively

Detailed contents of each spots see the ESM Table S2-2

(detailed in ESM Table S2-2). Iron (Fe) has the largest variation for the six sphalerite samples. However, except for sulfur (S) and zinc (Zn), other elements have low and scattered contents.

The DBS shows significantly higher contents of Fe than the LBS, which is similar with their deviation results of IR microthermometric fluid inclusion data. In addition, in the three plates separated from the same section, the Fe contents show a consistently positive correlation with the deviations of IR microthermometric data (Fig. 4; ESM Tables S2-10 and S2-11). Furthermore, the black area in

DBS with a much lower IR transmittance has a higher average Fe content of 2.3 wt% (Fig. 4b).

Wolframite

The major, minor, and trace element contents of wolframite were measured by EPMA, and 15 spots were analyzed in each wolframite samples to calculate the average contents. The results are listed in Table 2 and detailed in ESM Table S2-3. The average contents of FeO and MnO of the

Table 2 Average contents of major, minor, and trace elements of wolframite (wt%), measured by EPMA

Sample no.	Spot	MnO	FeO	WO ₃	SiO ₂	Ta ₂ O ₅	ZrO ₂	Nb ₂ O ₅	HfO ₂	SnO ₂	TiO ₂	Total
JGXS-1	15	15.10	10.22	74.57	0.33	0.26	bdl	0.14	bdl	bdl	bdl	100.62
JGXS-2	15	15.36	9.85	75.00	0.35	0.29	bdl	0.16	bdl	bdl	bdl	101.01
JGXS-3	15	15.15	10.29	74.92	0.39	0.29	bdl	0.12	bdl	bdl	bdl	101.16
YGX-1	15	9.72	15.25	75.47	0.33	0.29	bdl	bdl	bdl	bdl	bdl	101.06
YGX-2	15	9.74	15.06	75.11	0.37	0.28	bdl	bdl	bdl	bdl	bdl	100.56
YGX-3	15	9.61	15.31	75.24	0.37	0.29	0.06	bdl	bdl	bdl	bdl	100.88

bdl below the detection limit

Detailed contents of each spots see the SEM Table S2-3

three Yaogangxian wolframites are 15.06 to 15.31 wt% and 9.61 to 9.74 wt%, respectively, whereas three Jiagangxueshan wolframites yielded 9.85 to 10.29 wt% for FeO and 15.10 to 15.36 wt% for MnO.

Stibnite

The results of major, minor, and trace element contents of stibnite are listed in Table 1 with detailed results in ESM Table S2-2. Arsenic, lead, and gold show the largest and highest variation in concentration, whereas all the other elements have contents lower than 0.1 wt% (Table 1).

Pyrite

The EPMA results of major, minor, and trace elements of pyrite are listed in Table 1 with detailed results in ESM Table S2-2. Except for Fe, S, Pb, and Bi, the contents of other elements are below detection limit. The contents of the detected elements do not show significant difference in the pyrite samples.

Discussion

Factors excluded for IR light energy absorption

Our experiments were designed to investigate the possible factors affecting the absorption of IR energy, which include mineral types, fluid inclusion chemistry (salinity, H₂O, and CO₂), duration of illumination, effect of the silver lid in the Linkam stage, relative IR light intensity, and field iris diaphragm size (Campbell and Robinson-Cook 1987; Campbell 1991; Rosière and Rios 2004; Lüders 2017). Based on the experimental results, we find that fluid inclusion chemistry, illumination time, and presence of a silver lid have no effect in absorption of IR energy.

The IR microthermometric results of two-phase liquid-rich pure H₂O and three-phase CO₂-rich synthetic fluid inclusions showed small deviations, mostly within analytical error of the Linkam freezing/heating stage. In addition, the three-phase CO₂-rich and the two-phase liquid-rich fluid inclusions in quartz from the Majiayao and Jiagangxueshan deposits yielded the same deviations (ESM Tables S2-6 and S2-7). Hence, even though H₂O and CO₂ have a strong absorption band in IR light (Campbell and Robinson-Cook 1987; Campbell 1991), the two cases effectively prove that the presence of H₂O and CO₂ in fluid inclusions do not have any effect in absorbing IR energy, or that warming are within precision of the freezing/heating stage. The parallel curves of measured data indicate that fluid inclusions with different

salinities (Figs. 3b, c; 6a) or with different compositions, e.g., H₂O–NaCl and H₂O–NaCl–CaCl₂ (Fig. 4a) yielded almost the same deviations of microthermometric results caused by IR radiation. These results suggest that the ions in the fluid inclusions, which are expressed as salinity, do not have any effect on IR energy absorption.

The possible heating effect of the silver lid in the Linkam stage was proposed by Lüders (2017). However, our measurements of several fluid inclusions in wolframite with or without a silver lid yielded similar deviations of IR microthermometric data (Fig. 3d; ESM Table S2-14), and therefore we infer that the silver lid does not have any major influence on IR microthermometry. The role of the silver lid in the Linkam stage is to reduce the difference in temperature between the sample stage and the ambient air, and to obtain more accurate temperatures of phase changes.

No temperature variation was observed in hematite during IR analysis, even under IR light exposure longer than 1 h during measurements in the study of Rosière and Rios (2004). This was thought to be the evidence that IR light did not have influence on their microthermometric results. During measurements of T_m of fluid inclusions hosted in different minerals, we measured some fluid inclusions twice with different rates of heating, and we found no difference between the two measurements (ESM Table S2-15). Moreover, in T_m measurements under an IR intensity of 10, when it was close to the total melting of ice with a bubble and a small remnant ice in the inclusion and temperature was constant, we reduced the IR intensity or changed from IR light to visible light and observed that the volume of ice became larger (Fig. 7). The ice was stable at a new size after the light setting was changed, no matter how long it was exposed to IR radiation. These observations indicate that the absorption of IR light energy and deviation of IR microthermometric data are only function of IR light intensity, and are not related to illumination time.

Mineral type: a controlling factor for deviations of IR microthermometry

Our microthermometric results of fluid inclusions studied under visible and IR light show that the IR radiation can lower the phase change temperature, which is consistent with previous studies for opaque minerals (Moritz 2006; Ge et al. 2011; Casanova et al. 2018). In addition, we document that fluid inclusions hosted by different minerals show different deviations of IR microthermometric results, caused by IR radiation.

Our careful and accurate measurements indicate that even fluid inclusions in quartz absorb some IR energy and result in lower apparent temperature of phase change (ESM Tables S2-6–S28). Furthermore, variations in ice volume in fluid

inclusions, when the light was changed from IR intensity of 10 to visible light (Fig. 7a–c), show that quartz samples from the Majiayao, Jiagangxueshan, and Yaogangxian deposits absorbed IR energy. The Majiayao quartz sample absorbed more IR energy than the Jiagangxueshan and Yaogangxian quartz samples.

Microthermometric temperature measurements in a fluorite sample are unaffected by IR light. In contrast, measurements of fluid inclusions in sphalerite samples (DBS and LBS) show variable deviations, in which one group of fluid inclusions has the largest deviation (4.3 °C). Combined with quartz, it seems that even transparent to translucent minerals can absorb the energy of IR light, with variable degrees. Thus, it is reasonable to infer that the phenomenon of minerals absorbing IR radiation energy is more common than what was thought before.

Since pyrite has a lower band gap energy and a higher IR absorption edge (Campbell et al. 1984; Campbell 1991; Lüders 2017), it can be expected that pyrite absorbs more IR energy than wolframite and stibnite, and results in a higher deviation of IR microthermometric results. However, our IR microthermometric results in pyrite from the Yinjiagou and Linglong deposits show relatively small deviations (Fig. 3c; ESM Table S2-13). Figure 7 d–f compare the ice volume change in fluid inclusions in the Yaogangxian wolframite with a 9.0 °C deviation, in Xikuangshan stibnite with a 4.6 °C deviation and in Yinjiagou pyrite with a 3.1 °C deviation, when changing the setting from IR10 to IR8. The ice volume change of the fluid inclusion in Yinjiagou pyrite was smaller than that in Xikuangshan stibnite or Yaogangxian wolframite. These observations further confirm that pyrite absorbed limited IR energy and also suggest that different minerals can absorb IR energy variously, which is consistent with the relatively lower deviation of IR microthermometric results of fluid inclusions hosted by pyrite compared with wolframite, enargite, and stibnite (Casanova et al. 2018).

The FTIR spectra contain significant information about the variable capacity of these minerals in absorbing IR energy. Wolframite shows two IR absorption edges and two maxima of IR transmittance in the FTIR spectra (Fig. 8; Bailly et al. 2002; Lüders 2017). The two absorption edges start at a wavelength lower than 1 µm and of 1.7 to 1.8 µm. Due to the existence of the first peak of IR transmittance at a short wavelength, the wolframite can be studied using a CCD camera with a short spectral response range (0.8–1.1 µm). However, pyrite has only one absorption edge at ca. 1.3 to 1.4 µm (Fig. 8; Lüders and Ziemann 1999), which corresponds to its

relatively low band gap energy. In the spectral range of 1.3 to 1.8 µm, pyrite has a much higher IR transmittance than wolframite. The difference of IR transmittance at this range should be the key to answer why pyrite, with a low band gap energy, exhibits relatively low deviations of IR microthermometric data. Stibnite has a relatively low IR transmittance and an absorption edge lower than 1 µm (Fig. 8; Lüders 2017). It may be that the relatively low IR transmittance of stibnite in the near-IR range makes some stibnite samples yield higher deviations than pyrite in the IR microthermometric experiments (Fig. 7d–f). The FTIR spectrum of enargite shows a relatively low IR transmittance of 10% in the whole near-IR range (Lüders 2017). This can explain the large temperature deviation of 15 °C between the IR2 and IR12 settings in the study of Moritz (2006), although enargite has a relatively higher band gap energy than pyrite. Hence, there is no consistent correlation between the band gap energy and the IR absorption capacity of minerals. Compared with minerals with a low band gap energy (e.g., pyrite), fluid inclusions in minerals with relatively high band gap energy (e.g., enargite, Fe-rich wolframite, and sphalerite) are more susceptible to variations of the temperature of phase change.

Elemental substitutions within mineral: a key factor influencing IR energy absorption of minerals

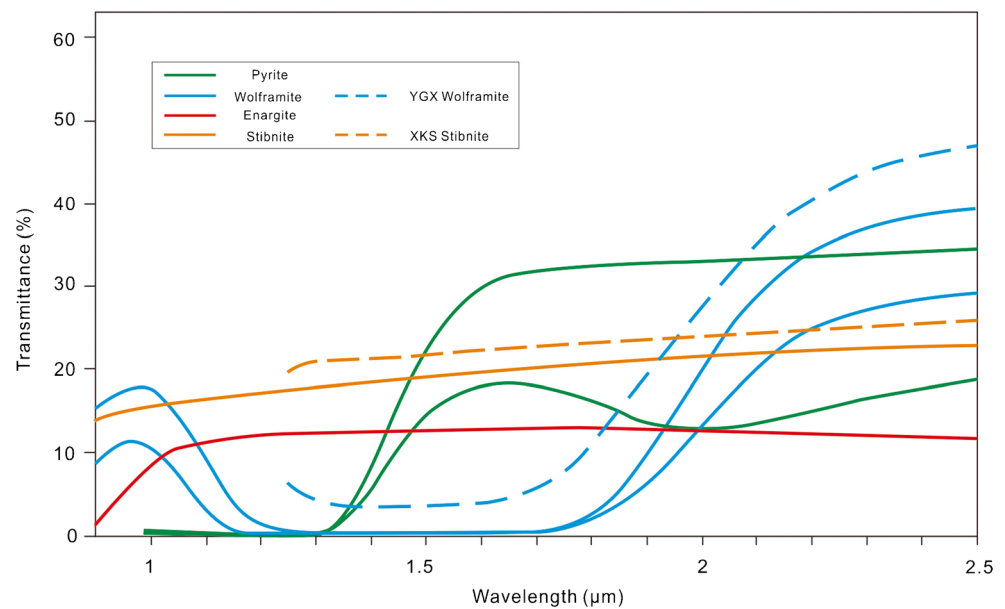
As discussed above, the host mineral of fluid inclusions is the critical factor controlling the different degrees of phase change temperature variations caused by IR light. We also document different variations of IR microthermometric results for fluid inclusions hosted in the same mineral from different samples or deposits, and even fluid inclusions from different parts within the same mineral section.

Iron substitution in sphalerite

The influence of Fe content on the IR transmittance of sphalerite was highlighted by Lüders (2017). In the present study, IR microthermometric temperature variations correlate with FTIR spectra and Fe contents of sphalerite. Sphalerite with a higher Fe content yields larger deviation of IR microthermometric data and a lower IR transmittance in FTIR spectra. This co-variation is observed in DBS and LBS, and in different areas (DBS-1, DBS-2, DBS-3, DBS-black or LBS-1, LBS-2, LBS-3) from the same sphalerite section (Fig. 4; Table 1).

The correlation of Fe contents with the physical features of sphalerite indicates that the Fe content controls the behavior of sphalerite under IR light. The incorporation of Fe reduces the IR transmittance of sphalerite and increases its absorption of

Fig. 8 Compilation of FTIR spectra of wolframite (Lüders 2017 and Yaogangxian wolframite), pyrite (Lüders and Ziemann 1999), enargite (Lüders 2017), and stibnite (Lüders 2017 and Xikuangshan stibnite)



IR energy. Previous IR studies that reported absence of variation of microthermometric data can possibly be explained by the Fe-poor sphalerite samples, as the sphalerite fluid inclusions could also be measured under visible light (Campbell and Panter 1990; Bailly et al. 2000, 2002; Shimizu et al. 2003; Shimizu and Morishita, 2012). However, the possible variation of IR microthermometric results for fluid inclusions hosted by Fe-rich sphalerite should not be neglected (e.g., up to 8.99 wt% Fe, Shimizu and Morishita 2012).

Iron substitution in wolframite

The control of the concentration of Fe on the IR transparency of wolframite was discussed in previous studies, as the incorporation of Fe influences the transparency of wolframite in visible light (Campbell 1991; Bailly et al. 2002). Our wolframite samples from the Jiagangxueshan and Yaogangxian deposits have compositions between the ferberite (FeWO_4) and huebnerite (MnWO_4) end-members. The Yaogangxian wolframite has higher Fe contents (close to ferberite) compared to the Jiagangxueshan wolframite (Table 2). The former yielded larger deviations of the microthermometric fluid inclusion data under IR light, lower IR transmittance, and longer IR absorption edge than the Jiagangxueshan samples (Fig. 5; ESM Tables S2-4 and S2-5). In addition, among the different samples of wolframite of the same deposit studied for fluid inclusions, the sample with the lowest FeO content

yielded the microthermometric results with the smallest phase change temperature variations (Table 2, ESM Tables S2-4 and S2-5).

The co-variations of IR microthermometric data, IR transmittance, and EPMA results indicate that the Fe content controls the absorption of IR energy on wolframite, which is consistent with the results of the in situ analyses of wolframite (Bailly et al. 2002; Ortelli et al. 2018). In summary, fluid inclusion temperatures acquired during IR microthermometry will be more variable in Fe-rich wolframite and ferberite in contrast to huebnerite. Hence, the possible influence of IR light on microthermometric results of fluid inclusions hosted by wolframite must be taken into account.

Trace element substitution in quartz

The study also documents variations in IR microthermometric results for fluid inclusions hosted by quartz. The deviations of IR microthermometric results are the largest in the quartz samples from Majiayao deposit, which have the highest P and Ca concentrations. In contrast, the deviations are smaller for inclusions in the Yaogangxian samples, which have lower P and Ca contents. The contents of Li, Al, and Ti are the highest in the Jiagangxueshan samples and the lowest in the Majiayao samples. But the variations in the concentration of these elements are relatively small (ESM Table S2-1). Thus, we speculate that the elemental concentrations (e.g., Al, P, and Ca) in

quartz might account for the variations of inclusion data in quartz from the three deposits.

Minor and trace element substitution in stibnite

The EPMA results of stibnite with different deviations of IR microthermometric data indicate that As, Pb, and Au have varying contents in the host stibnite samples (Table 1). These three elements usually show a geochemical affinity in stibnite-gold deposits, including the Xikuangshan and Qinglong deposits (Groves et al. 1998; Hagemann and Lüders 2003; Yang et al. 2006; Chen et al. 2018). It is more probable that the variation of As content contributes to the observed deviation of IR analyses of fluid inclusions in stibnite, although the role of other elements cannot be ruled out.

Minor and trace element substitution in pyrite

The effect of decreasing IR transparency caused by substitution of trace elements in pyrite (e.g., As, Cu, and Co) was discussed in previous studies (Richards and Kerrich 1993; Kouzmanov et al. 2002; Ortelli et al. 2018). We document slightly different degrees of deviations of IR microthermometric data (Fig. 3c; ESM Table S2-13), but As, Cu, and Co contents are below detection limit (Table 1). The analytical domains for EPMA were chosen in the same areas of the measured fluid inclusions, and these regions had good IR transparency (Fig. 2i), in which no compositional changes are detected by EPMA.

A solution: infrared microthermometry with smallest diaphragm opening

Accurate microthermometric fluid inclusion data are fundamental and a prerequisite for understanding the evolution and source of hydrothermal fluids. Since the temperature of phase change decreases with increasing IR light intensity, working with the lowest possible IR light intensity and the smallest diaphragm opening was suggested to minimize the deviation of IR microthermometry (Moritz 2006). However, the lowest IR light intensity does not mean complete absence of IR absorption. For example, the lowest IR light intensity (2) was used with the largest diaphragm opening. On the other hand, when the smallest diaphragm was used, the lowest intensity was set at 3. In other cases, when the IR transparency of the host mineral was poor, the setting of IR light intensity was higher (5). Furthermore, when working with fluid inclusions hosted in pyrite or other minerals with relatively low band gap energies, a tube-type camera such as the Dage-MTI LSC-70, which has a long spectral response but lower

spatial resolution was required. This would require the use of higher IR light intensities (e.g., 8 or 10) for better observations of phase changes.

In the present study, we acquired the true values of phase change temperatures of fluid inclusions hosted by opaque minerals, using the improved cycling method (Fig. 1). Hence, the deviations in the IR microthermometry of fluid inclusions could be evaluated quantitatively. When using the smallest diaphragm opening and the lowest IR light intensity (3), the deviation of IR microthermometric measurements on wolframite fluid inclusions were 0 to 0.2 °C, which results in an overestimation of the fluid inclusion salinity by 0 to 0.4 wt% NaCl equivalent (ESM Tables S2-4 and S2-5). However, using an IR light intensity of 5 with the smallest diaphragm opening, the deviations are 0.2 to 0.6 °C, which is equivalent to an overestimate of salinity of 0.3 to 0.9 wt% NaCl equivalent. Fluid inclusions in stibnite yielded smaller temperature deviations during IR microthermometry, consequently resulting in smaller salinity overestimates.

Even though our IR microthermometric data on fluid inclusions in pyrite exhibit relatively small deviations, a relatively high IR light intensity was required. When measuring with the smallest diaphragm opening, we needed to use an IR light intensity of 5 to observe the phase change. The deviations were 0.1–0.2 °C and the calculated variations in salinity are almost negligible, which is similar to the results of Zhu et al. (2013).

In line with the study by Moritz (2006), our quantitative studies show that using the lowest possible IR light intensity with the smallest diaphragm opening can diminish the variations of phase change temperatures caused by IR radiation in various ore minerals. Therefore, the phase change temperatures acquired under such condition are closer to the true values. However, when a high-intensity IR light was used, the possible variation of fluid inclusion data should not be neglected, and the improved cycling method (Fig. 1) would be helpful to obtain the most accurate temperature data.

Conclusions

The absorption of IR energy by minerals is more common than reported before, which has implications for fluid inclusion data gathered by IR microthermometry. The transparent to translucent minerals (e.g., quartz, sphalerite) also absorb IR energy, which has an impact on the temperatures of phase changes measured under IR light.

Some factors considered before (e.g., fluid inclusion chemistry, presence of the silver lid, illumination time) do not have an effect on absorbing IR energy and decreasing the

temperature measured under IR light. The nature of the host mineral seems to be the most important factor. Minerals with a low band gap energy (e.g., pyrite) may absorb limited IR energy. Hence, there is no consistent correlation between the band gap energy of minerals and its capacity in absorbing IR energy. The deviation of fluid inclusion data hosted by minerals with relatively high band gap energy should not be ignored (e.g., Fe-rich sphalerite, wolframite).

Substitution of major or trace elements in minerals can influence the degree of absorbance of IR energy and the variation of fluid inclusion data. The Fe substitution increases the degree of absorbing IR energy in wolframite and sphalerite. Variable contents of trace elements may play a role in controlling IR energy absorption in quartz and stibnite (i.e., substitution of As in stibnite and Al, P, and Ca in quartz). However, additional *in situ* trace elemental analyses are needed to constrain the correlation among the substitution of trace elements, the variation of IR microthermometry, and absorption of IR energy.

Using the lowest possible IR light with the smallest diaphragm opening is recommended to minimize the “warming effect” of IR light. However, if high IR light intensity is necessary for observation, the improved cycling method proposed in our study enables more precise microthermometric measurements.

Acknowledgments We thank Drs. Wen-Chao Su, Ming-Tian Zhu, Yang Shen, Xi-Feng Mi, and Kai Feng for their help in the sample collection. Thanks are also given to Dr. Ting-Guang Lan for his assistance in the LA-ICP-MS analyses of quartz, Ms. Di Zhang for her aid in the EPMA experiments, and Ms. Lin Chen for his help in the FTIR experiments. Dr. T. James Reynolds is thanked for his thoughtful comments and constructive suggestions. Editor-in-Chief Dr. Georges Beaudoin, Associate Editor Dr. Robert Moritz, Dr. Andrew Campbell, and Dr. Toru Shimizu are thanked for their constructive and valuable comments which greatly contributed to the improvement of the manuscript.

Funding information This study was funded by the National Key Research and Development Program of China (2016YFE0203000) and the National Natural Science Foundation of China (41672094).

References

- Bailly L, Bouchot V, Beny C, Milesi JP (2000) Fluid inclusion study of stibnite using infrared microscopy: an example from the Brouzils antimony deposit (Vendee, Armorican Massif, France). *Econ Geol* 95:221–226
- Bailly L, Grancea L, Kouzmanov K (2002) Infrared microthermometry and chemistry of wolframite from the Baia Sprie Epithermal deposit, Romania. *Econ Geol* 97:415–423
- Campbell AR, Hackbarth CJ, Plumlee GS, Petersen U (1984) Internal features of ore minerals seen with the infrared microscope. *Econ Geol* 79:1387–1392
- Campbell AR, Robinson-Cook S (1987) Infrared fluid inclusion microthermometry on coexisting wolframite and quartz. *Econ Geol* 82:1640–1645
- Campbell AR, Panter KS (1990) Comparison of fluid inclusion in coexisting (cogenetic) wolframite, cassiterite and quartz from St-Michaels Mount and Cligga Head, Cornwall, England. *Geochim Cosmochim Acta* 54:673–681
- Campbell AR (1991) Geologic applications of infrared microscopy. Society of Sedimentary Geologists (SEPM) Short Course, pp 161–171
- Casanova V, Kouzmanov K, Audétat A, Wälle M, Ubrig N, Ortelli M, Fontboté L (2018) Fluid inclusion studies in opaque ore minerals: II. A comparative study of synthetic fluid inclusions hosted in quartz and opaque minerals. *Econ Geol* 113:1861–1883
- Chen J, Yang RD, Du LJ, Zheng LL, Gao JB, Lai CK, Wei HR, Yuan MG (2018) Mineralogy, geochemistry and fluid inclusions of the Qinglong Sb-(Au) deposit, Youjiang basin (Guizhou, SW China). *Ore Geol Rev* 92:1–18
- Ge X, Su WC, Zhu LY, Wu LY (2011) A study on the influence of infrared light source intensity on salinity of fluid inclusion in opaque mineral by using infrared microthermometry: in the case of stibnite. *Acta Mineral Sin* 31:366–371 (in Chinese with English abstract)
- Goldstein RH, Reynolds TJ (1994) Society of Sedimentary Geologists (SEPM) Short Course. In: Systematics of fluid inclusions in Diagenetic minerals
- Groves DI, Goldfarb RJ, Gebre-Mariam M, Hagemann SG, Robert F (1998) Orogenic gold deposits: a proposed classification in the context of their crustal distribution and relationship to other gold deposit types. *Ore Geol Rev* 13:7–27
- Hagemann SG, Lüders V (2003) P-T-x conditions of hydrothermal fluids and precipitation mechanism of stibnite-gold mineralization at the Wiluna lode-gold deposits, Western Australia: conventional and infrared microthermometric constraints. *Mineral Deposita* 38:936–952
- Korges M, Weis P, Lüders V, Laurent O (2018) Depressurization and boiling of a single magmatic fluid as a mechanism for tin-tungsten deposit formation. *Geology* 46:75–78
- Kouzmanov K, Bailly L, Ramboz C, Rouer O, Bény JM (2002) Morphology, origin and infrared microthermometry of fluid inclusions in pyrite from the Radka epithermal copper deposit, Srednogie zone, Bulgaria. *Mineral Deposita* 37:599–613
- Kouzmanov K, Pettke T, Heinrich CA (2010) Direct analysis of ore-precipitating fluids: combined IR microscopy and LA-ICP-MS study of fluid inclusions in opaque ore minerals. *Econ Geol* 105:351–373
- Lindaas SE, Kulis J, Campbell AR (2002) Near-infrared observation and microthermometry of pyrite-hosted fluid inclusions. *Econ Geol* 97:603–618
- Lüders V, Ziemann M (1999) Possibilities and limits of infrared light microthermometry applied to studies of pyrite-hosted fluid inclusions. *Chem Geol* 154:169–178
- Lüders V (2017) Contribution of infrared microscopy to studies of fluid inclusions hosted in some opaque ore minerals: possibilities, limitations, and perspectives. *Mineral Deposita* 52:663–673
- Moritz R (2006) Fluid salinities obtained by infrared microthermometry of opaque minerals: implications for ore deposit modeling - a note of caution. *J Geochem Explor* 89:284–287
- Ni P, Wang XD, Wang GG, Huang JB, Pan JY, Wang TG (2015) An infrared microthermometric study of fluid inclusions in coexisting quartz and wolframite from late Mesozoic tungsten deposits in the Gannan metallogenic belt, South China. *Ore Geol Rev* 65:1062–1077

- Ortelli M, Kouzmanov K, Wälle M, Ubrig N, Casanova V (2018) Fluid inclusion studies in opaque ore minerals: I. Trace element content and physical properties of ore minerals controlling textural features in transmitted near-infrared light microscopy. *Econ Geol* 113:1845–1860
- Richards JP, Kerrich R (1993) Observations of zoning and fluid inclusions in pyrite using a transmitted infrared light microscope ($\lambda \leq 1.9 \mu\text{m}$). *Econ Geol* 88:716–723
- Roedder E (1984) Fluid inclusions: reviews in mineralogy. *Mineralog Soc Amer*:1–644
- Rosière CA, Rios FJ (2004) The origin of hematite in high-grade iron ores based on infrared microscopy and fluid inclusion studies: the example of the Conceicao mine, Quadrilatero Ferífero, Brazil. *Econ Geol* 99:611–624
- Shimizu T, Aoki M, Kabashima T (2003) Near-infrared and visible microthermometry of fluid inclusions in sphalerite from a possible southeast extension of the Toyoha Polymetallic deposit, Japan. *Resour Geol* 53:115–126
- Shimizu T, Morishita Y (2012) Petrography, chemistry, and near-infrared microthermometry of indium-bearing sphalerite from the Toyoha polymetallic deposit, Japan. *Econ Geol* 107:723–735
- Takács Á, Molnár F, Turi J, Mogessie A, Menzies JC (2017) Ore mineralogy and fluid inclusion constraints on the temporal and spatial evolution of a high-sulfidation epithermal Cu-Au-Ag deposit in the Reesk ore complex, Hungary. *Econ Geol* 112:1461–1781
- Wei WF, Hu RZ, Bi XW, Peng JT, Su WC, Song SQ, Shi SH (2012) Infrared microthermometric and stable isotopic study of fluid inclusions in wolframite at the Xihuashan tungsten deposit, Jiangxi province, China. *Mineral Deposita* 47:589–605
- Wilkinson JJ (2001) Fluid inclusions in hydrothermal ore deposits. *Lithos* 65:229–272
- Yang DS, Shimizu M, Shimazaki H, Li XH, Xie QL (2006) Sulfur isotope geochemistry of the supergiant Xikuangshan Sb deposit, Central Hunan, China: constraints on sources of ore constituents. *Resour Geol* 56:385–396
- Zhu MT, Zhang LC, Wu G, He HY, Cui ML (2013) Fluid inclusions and He-Ar isotopes in pyrite from the Yinjiagou deposit in the southern margin of the North China Craton: a mantle connection for polymetallic mineralization. *Chem Geol* 351:1–14

Publisher's note Springer Nature remains neutral with regard to jurisdictional claims in published maps and institutional affiliations.